Stability and electronic structure of the complex K_2PtCl_6 structure-type hydrides

S.V. Halilov and D.J. Singh

Center for Computational Materials Science,
Naval Research Laboratory, Washington, DC 20375-5000, USA

M. Gupta

Thermodynamique et Physico-Chimie d'Hydrures et Oxydes, EA3547, Batiment 415,
Science des Materiaux, Universite Paris-Sud, 91405 Orsay, France

R. Gupta

Service de Recherches de Metallurgie Physique, Commissariat a l'Energie Atomique, Centre d'Etudes de Saclay,
91191 Gif Sur Yvette Cedex, France
(February 2, 2008)

The stability and bonding of the ternary complex K_2PtCl_6 structure hydrides is discussed using first principles density functional calculations. The cohesion is dominated by ionic contributions, but ligand field effects are important, and are responsible for the 18-electron rule. Similarities to oxides are discussed in terms of the electronic structure. However, phonon calculations for Sr_2RuH_6 also show differences, particularly in the polarizability of the RuH_6 octahedra. Nevertheless, the yet to be made compounds Pb_2RuH_6 and Be_2FeH_6 are possible ferroelectrics. The electronic structure and magnetic properties of the decomposition product, $FeBe_2$ are reported. Implications of the results for H storage are discussed.

I. INTRODUCTION

The complex hydrides, DMH_6, D=Mg,Ca,Sr,Eu and M=Fe,Ru,Os form in the cubic ($Fm3m$,#225), K_2PtCl_6 structure.[1–6] This structure has D on site $8c$ (1/4,1/4,1/4), M on $4a$ (0,0,0), and H on site $24e$ (x_H,0,0). These compounds are of fundamental interest because of the unusual structural motif and the interest in understanding resulting electronic structure, and the bonding associated with it. Furthermore, they could be of practical interest as potential hydrogen storage materials. Mg_2FeH_6 has very high volume and mass storage efficiency (150 g/l and 5.4 wt. %), but is too stable for reversible room temperature applications.[5,7,8] In this regard, understanding of the electronic structure and cohesion may be helpful in finding modifications that improve the thermodynamics, to produce a material for hydrogen storage in mobile applications.

The crystal structure may be regarded as a cubic double perovskite $A_2BB'H_6$, with $A = D$, B=M and B'=vacancy. Therefore, from a structural point of view, the compounds consist of MH_6 octahedra, well separated by presumably inert D ions, whose role is to fill space and donate charge to the MH_6 units. The cubic $Fm3m$ structure is maintained for all these compounds in spite of large variations of the A and B site cation radii, in contrast to the structural distortions often found in oxide perovskites and double perovskites.

These compounds are insulators, and, like many of the complex hydrides,[5] follow the 18 electron rule, which says that the number of non-bonded metal electrons plus the number of electrons in the metal-ligand bonds should be 18. In the simplest view, this would correspond to full s, p and d shells associated with the $[MH_6]^{4-}$ structural units. However, Miller and co-workers,[9] have emphasized the importance of ligand field effects in these complex hydrides, and, in fact, the calculated electronic structures for these materials show band gaps within the d manifolds, indicating a more complex situation.[11] In particular, insulating band structures, in qualitative accord with experiment, resulting from band gaps between crystal field split transition metal d manifolds were found in non-self-consistent warped muffin-tin calculations, based on the $X\alpha$ method with $\alpha = 1$.

Here, we re-examine the electronic structures, which we obtain using a full-potential, self-consistent linearized augmented planewave (LAPW) method, and use these results, along with calculations of the formation enthalpies, to discuss the bonding of these materials and possible directions for modifying them to alter their stability. In addition we discuss the hypothetical materials, Pb_2RuH_6, which was studied as a potential ferroelectric, and Be_2FeH_6, which is both in relation to ferroelectricity and to better understand their stability.

II. APPROACH

As mentioned, the calculations were done within the local density approximation (LDA) using the general potential linearized augmented planewave (LAPW) method.[12] Local orbital extensions[13] were used to relax the linearization errors for the transition metal d states, and to treat the upper semicore levels of the

alkaline earth and transition metal atoms. An LAPW sphere radius $r_H = 1.1$ a_0 was used for H in all the compounds. Metal radii of 1.8 a_0 were used for Mg_2FeH_6 and Ca_2FeH_6. For Sr_2FeH_6, metal radii, $r_{Sr} = 2.0$ a_0 and $r_{Fe} = 1.8$ a_0 were used for Sr and Fe, respectively. For Ca_2RuH_6 and Sr_2RuH_6, metal radii of 1.95 a_0 were used. For Mg_2RuH_6 we used $r_{Mg} = 1.8$ a_0 and $r_{Ru} = 1.9$ a_0. Well converged basis sets, defined by $r_H G_{max} = 6.0$, where G_{max} is the planewave cut-off were employed. The Brillouin zone sampling during the iteration to self-consistency was done using the special-**k** points method with a $4 \times 4 \times 4$ mesh, which corresponds to 10 **k**-points in the irreducible wedge. Densities of states were generated using a tetrahedron mesh of 145 **k** points in the wedge. Convergence was tested, both for the zone sampling and basis set size, by repeating some calculations with higher $r_H G_{max} = 7$ and more **k** points ($8 \times 8 \times 8$). Based on these tests, the present convergence with respect to these parameters is better than 2 mRy/cell for total energies, and better than 1 mRy for band energies.

III. ELECTRONIC STRUCTURE AND THE EIGHTEEN ELECTRON RULE

Crystal field effects, which are important here, may be expected to be sensitive to the H positions. Here we use LDA relaxation to determine the H positions (given in Table I). As may be seen, they are in good agreement with experiment for those compounds for which neutron refinements are available. Table I also gives the full symmetry A_g Raman phonon frequency associated with the H internal structural parameter. Raman and inelastic neutron scattering measurements[14] for Mg_2FeH_6 yield an experimental frequency of 1873 cm^{-1}, in good agreement with the present LDA value of 1923 cm^{-1}. The LDA frequencies follow the reported trend for H bond stretching modes in infrared data,[5] decreasing with increasing D ionic radius, and increasing with increasing M atomic number. It is interesting to note the increase in frequency from Sr_2RuH_6 to Sr_2OsH_6. Generally, the ionic properties of $4d$ and $5d$ elements are very similar due to relativistic contraction. The main difference, which is also due to relativistic contraction, is that the s states are lower relative to the d states in the $5d$ series. This leads to a higher position of the d states relative to ligand states in compounds where the transition elements are cations. The result is reduced covalency. Since covalency softens ionic interactions, the result is a stiffer lattice in $5d$ ionic compounds relative to the corresponding $4d$ compounds. A good example is the comparison of $KNbO_3$, which is a good ferroelectric with $KTaO_3$, which has practically the same lattice parameter, but is not ferroelectric.[10]

The calculated electronic band structures are shown in Figs. 1, 2 and 3. The corresponding electronic densities of states (DOS) are in Figs. 4, 5 and 6. The electronic structures are qualititively similar to those of Orgaz and Gupta (Ref. 11), in that all the materials are insulating with band gaps within the transition metal d bands.

The band structure for all the compounds studied consists of 6 H $1s$ derived bands, holding 12 electrons, followed by crystal field split transition metal d bands. The $1s$ band width is largest in the Mg compounds, and in the case of Mg_2RuH_6 this is sufficient to yield an overlap between the $1s$ manifold and the lower d manifold. In the octahedral crystal field of the H, the metal d bands separate into a 3-fold degenerate (6 electrons) t_{2g} manifold and a 2-fold degenerate (4 electrons) e_g manifold. The 18 valence electrons then populate the H derived $1s$ bands and the metal t_{2g} bands; the insulating gap is between the occupied t_{2g} and the unoccupied e_g manifolds. Since these are gaps within a crystal field split d-band, LDA band gap errors are expected to be small in the absence of strong correlation effects.[15] However, we note that the gap is between narrow d bands, and so a larger gap may be observed both because of optical dipole selection rules and, in the Fe compounds, correlation effects.

The H $1s$ character of the lowest 6 bands may be seen from the projections of the DOS onto the LAPW spheres. The small 1.1 a_0 H spheres, used here, imply that most of the charge of H ions will be outside the sphere. A free H^- ion, stabilized by a Watson sphere (to approximately represent the Madelung field) of radius 3.01 Å, would have only 0.45 e (of 2) inside a sphere of radius 1.1 a_0. Integrating the H s projection of the DOS over the lowest 6 bands, we obtain from 0.50 e (Ca_2RuH_6 and Sr_2RuH_6) to 0.52 e (Sr_2FeH_6) inside each H sphere, not far from this simple ionic view especially if one allows for a somewhat different breathing. This is also similar to what was found for $NaAlH_4$.[16] Thus the basic electronic structure is ionic consisting of H anions and D and M cations. These compounds should therefore be viewed as ionic for understanding the crystal cohesion.

However, from the stand-point of understanding the electronic structure and H storage properties, covalency is important. The effects of M – H hybridization are clearly seen in the electronic structures. While the bottom 6 bands are essentially H $1s$ bands, they contain the two formally bonding H s - M e_g σ combinations (as well as four non-bonding combinations). The lowest band is the symmetric combination of s orbitals, which is a non-bonding combination with M e_g states, but is formally bonding with the nominally unoccupied M s states. This is followed by five more H s bands, including the non-bonding and the formally bonding H s - M e_g σ combinations. In terms of degeneracies, this division into a "s"-like one fold symmetric band, a five-fold manifold and the three-fold t_{2g} manifold is formally like the s, p, d electron counting of the 18-electron rule. However, this counting does not correspond to atomic level filling. Instead, the 2-electron "s" and 10-electron "d" manifolds are actually from combinations of hydrogen s states, and are therefore very different in atomic character from the 6-electron, "p" group, which comes from very weakly hybridized M t_{2g} bands.

The lowest conduction bands derive mainly from the corresponding antibonding combinations and sd derived states associated with the D cation. The covalency in the $[MH_6]^{4-}$ units can be seen in the M d contributions to the H s bands, for example. The t_{2g} bands show much less hybridization, as expected in an octahedral ligand environment. It should be emphasized that the bands show relatively little dispersion, with the exception of the D=Mg compounds, and that there are generally clean gaps between the different manifolds (H s, t_{2g} and e_g), which implies that weakly interacting $[MH_6]^{4-}$ units may be regarded as the basic building blocks for understanding the band structure. The sizable crystal field splitting of the M d bands underlies the 18-electron rule in these compounds. In particular, without it the t_{2g} and e_g manifolds would overlap, and then there would be no barrier to adding more than 18 electrons; the 18 electron rule here is the result of the crystal field splitting of the metal d levels. The octahedral geometry, with its large ligand field is energetically favorable for 18 or fewer electrons.[17] The substantial crystal field splittings (as compared to the on-site Hund's coupling, which can be characterized by a Stoner $I \sim 0.7 - 0.9$ eV for Fe)[18,19] are responsible for the low spin Fe observed in these compounds.

To summarize the results so far, the electronic structure is built up in the following way in decreasing order of the size of the interactions involved. (1) Coulomb interactions, particularly the Madelung field, stabilize an ionic configuration, nominally $D^{2+}M^{4+}H_6^-$. This is the main ingredient in the cohesion. (2) Hybridization between the H s orbitals and the M e_g orbitals lead to a bonding anti-bonding splitting between these and contribute to a substantial crystal field splitting between weakly hybridized occupied M t_{2g} states and unoccupied M e_g states. This splitting and the position of the D derived states well above the t_{2g} energy underlies the 18 electron rule. (3) Hopping between the $[MH_6]^{4-}$ units (presumably mostly assisted hopping via unoccupied D s and d states) leads to band formation. This is reminiscent of some of the oxide double perovskites, $A_2MM'O_6$, with an inert M', such as Sr_2RuYO_6, although in that case the hybridization inside the $[RuO_6]^{7-}$ units is very much stronger than in the present hydrides.[20]

IV. PHONONS, FERROELECTRICITY AND HYPOTHETICAL Pb_2RuH_6

The resulting picture of ionic crystal with substantial covalency between anions and an octahedrally coordinated transition element cation suggests similarities with double perovskite oxides. Furthermore, the fact that the latttice contains a large anion (H$^-$) stabilized by the Madelung field and hybridized with nominally unoccupied transition metal states further suggests connections with perovskite oxides, particularly ferroelectrics. In fact, many of the technologically important ferroelectrics are based on perovskites ABO_3 with mixtures of metal atoms on the B sites (these can be disordered or ordered as in *e.g.* double perovskite). Examples include PZT [Pb(Zr,Ti)O$_3$], PMN-PT [Pb(Mg,Nb,Ti)O$_3$] and PZN-PT [Pb(Zn,Nb,Ti)O$_3$]. In these materials both Pb-O and B-O hybridization is important in the ferroelectricity.[31]

In order to further elucidate the relationship to oxides, we calculated those zone center phonon frequencies of Sr_2RuH_6 compatible with a rhombohedral $R32$ symmetry, and compare with similar calculations for hypothetical Pb_2RuH_6. This was done at the experimental lattice parameter of Sr_2RuH_6, using the relaxed H position. This non-centrosymmetric group would include the ferroelectric mode, if the material were ferroelectric. The calculations were done by fitting the dynamical matrix to a series of frozen phonon calculations with small displacements of the various atoms. This yields 6 three-fold degenerate modes (plus the three $\omega = 0$ acoustic modes). The frequencies and displacement patterns of the phonon modes are given in Table IV. The 2 % difference between the A_g frequencies for Sr_2RuH_6 between Tables I and IV reflect the different approaches and should be considered indicative of the errors in the fits used in constructing the dynamical matrix. The fitting errors can also be seen in the deviation of the mode character as given in Table IV from the A_g character required by symmetry. For the A_g frequency, the value in Table I should be considered more reliable because that value was obtained enforcing the exact mode symmetry, but it should be kept in mind that the LDA error is likely larger than the difference between the values in Tables I and IV.

The highest frequency branches correspond to H motions, as expected. Of these, the A_g Raman mode, which corresponds to symmetric breathing of the RuH$_6$ octahedra, is the stiffest mode, and the next lower mode also involves modulation of the Ru-H bond lengths. The two intermediate modes (738 cm^{-1} and 777 cm^{-1}) involve distortion of the octahedra, which would also yield lower frequency modes in oxides. The two lowest frequency modes are motions of the Sr atoms within their cages. The lowest mode is the antisymmetric motion of the Sr, which is not ferroelectric. The frequencies of these Sr motions are compatible with the frequencies of the shearing modes that modulate Sr-H distances when the mass difference is accounted for.

This pattern of phonon modes is quite different from what would occur in an oxide near ferroelectricity. In that case, there would be a low frequency cooperative mode. This would consist of a distortion where the cations move relative to the O atoms comprising the octahedra, reflecting the high polarizability of the octahedra softened by covalent interactions.[31,32] Here, the mode corresponding to motion of the Ru with respect to the H is at high frequency (1433 cm^{-1}) and the lower frequency Sr derived modes have only a small component of Ru motion relative to the H octahedra.

We repeated the calculations for the hypothetical compound Pb_2RuH_6. In perovskite and double perovskite

oxides, Pb typically can be substituted for Sr. The Pb compounds typically have unit cell volumes very close to the Sr analagues, but are more likely to be ferroelectric because of Pb-O covalency (e.g. $PbTiO_3$ vs. $SrTiO_3$). Since the experimental lattice parameter of Pb_2RuH_6 is unavailable, we used the value for Sr_2RuH_6. This choice also makes comparison of the two systems more direct. LDA relaxation of the lattice parameter yielded a value 1.8% smaller than this, but considering the usual underestimate of lattice parameters in the LDA, we do not consider the LDA value to be more reliable than the use of the Sr_2RuH_6 value.[33] The Pb_2RuH_6 modes (Table V) are qualitatively like those of Sr_2RuH_6, except that the low frequency Pb modes are shifted down in frequency. This shift is, however, larger than can be accounted for by the mass difference, and the modes are reversed in order. The lowest mode is now the symmetric mode and it is at zero frequency to within the precision of the present calculations. We also calculated the energy as a function of the rotation of the RuH_6 octahedron. Such rotational degrees of freedom compete with ferroelectricity in ferroelectrics such as $Pb(Zr,Ti)O_3$.[34] Here, these modes are stable. We obtain frequencies of 576 cm^{-1} and 490 cm^{-1}, for Sr_2RuH_6 and Pb_2RuH_6, respectively. This suggests Pb_2RuH_6 as a candidate ferroelectric hydride. We found a similar result for hypothetical Be_2FeH_6. In this case, we obtained a slightly unstable mode of Be character, with a ferroelectric displacement pattern, and stable rotational and antiferroelectric modes. If these compounds are made, the possibility of ferroelectricity should be investigated, *e.g.* by low temperature structural studies and temperature dependent dielectric measurements.

V. ENERGETICS AND ZERO POINT EFFECTS

In order to better understand the stability of these compounds, we performed calculations of the formation enthalpies by comparison of the total energies with those of decomposition products. Specifically, we did calculations for the elements, Mg,Sr,Ca,Fe,Ru and Os in their bulk metallic form (in the LDA at the experimental lattice parameters, parallel to the calculations done for the hydrides, including ferromagnetism for Fe), the H_2 molecule (relaxed, in the LDA) and MgH_2, CaH_2 and SrH_2 (using experimental lattice constants, but relaxed atomic positions). In addition calculations were done for elemental Be and the intermetallic phase Be_2Fe, which is the expected decomposition product of the hypothetical phase Be_2FeH_6 (see below).

For the H_2 molecule we used a cubic supercell of lattice parameter 4.5 Å. This yielded an LDA energy of -2.288 Ry, and bond length of 0.765 Å, and bond stretching vibrational frequency of 4217 cm^{-1}. These results are in good agreement with previous LDA calculations. For example, Patton and co-workers report a vibrational frequency of 4188 cm^{-1} and bond length of 0.765 Å.[21] The

H_2 zero point energy obtained from the LDA frequency is 25.2 kJ/mol. This is a substantial number, which underscores the fact[22-24] that zero point effects need to be considered in the thermodynamics of hydride formation. Here we neglect metal modes, and consider only the H contribution to the zero point energies, which we write as $3\hbar\bar{\omega}$ per H_2 unit, where $\bar{\omega}$ is an average H vibrational frequency. The effective $\bar{\omega}$ for H_2 is 703 cm^{-1}, so for hydrides with $\bar{\omega} > 703$ cm^{-1}, zero point motion will reduce the formation energy, and the corresponding deuterides and tritides will form more easily than the hydrides, while for materials with $\bar{\omega} < 703$ cm^{-1}, the converse will be true.[22] At least in principle, this difference can be used to obtain the average H frequency from experimental formation energies of hydrides and deuterides, but to our knowledge this has not been done for these materials.

In order to estimate $\bar{\omega}$ for the compounds considered here, we performed LDA calculations for selected distortions and assumed that the H behaves in an Einstein-like way. In particular, for MgH_2, we displaced a single H in the unit cell (which contains 4 equivalent H atoms) along the three principal directions in its cage and averaged the resulting frequencies to obtain an average frequency (the principal directions relative to the lattice are [1,$\bar{1}$,0], [1,1,0] and [0,0,1]). For CaH_2 and SrH_2, we used the average of the four full symmetry Raman modes that are H derived (there are two other such modes associated with metal motion). For the K_2PtCl_6 structure hydrides, we used the average of the highest two Γ-point modes consistent with rhombohedral symmetry (the highest of these is the full symmetry Raman breathing mode) to obtain an effective B-site metal – H bond stretching force constant (which contributes 1/3 of the modes) and obtained the effective force constant for the other two thirds of the modes by averaging the two other H derived modes from the rhombohedral symmetry and the octahedral rotation mode. As a test, we also calculated an average Einstein frequency for Mg_2FeH_6 by displacing a single H (of the six in the unit cell) perpendicular to the Fe-H "bond", and along it, similar to the procedure that was followed for MgH_2. This yielded a shear frequency of 727 cm^{-1} and a stretch frequency of 1828 cm^{-1}, for an average $\bar{\omega}=1094$ cm^{-1}, in fortuitously good agreement with the estimate of 1089 cm^{-1}, made as above (Table III). In all cases, the averages are arithmatical averages of frequencies as is appropriate for the zero point energy.

α-MgH_2 has a tetragonal structure (spacegroup $P4_2/mmm$) with one H coordinate, x. We obtain $x=0.3046$, in agreeement with the recent neutron measurement of Bortz and co-workers,[25] who obtained $x=0.3040$, and an LDA calculation by Yu and Lam,[26] who also obtained $x=0.304$. Moving a single hydrogen in the unit cell of MgH_2, we obtained frequencies of 1277 cm^{-1} along [1,1,0] (bond stretching) 592 cm^{-1} along [1,$\bar{1}$,0] (bond bending) and 993 cm^{-1} along [0,0,1] (mixed). The bond stretching "Einstein" frequency is near that of the full symmetry Raman mode, which we obtain at 1301 cm^{-1} and which is also of bond stretch-

ing character. This supports the simple Einstein-like approach used.

Good agreement with neutron diffraction results[27,28] is also obtained for the internal structural parameters of CaH_2 and SrH_2, which occur in an orthorhombic $Pnma$ structure, as given in Table II. As mentioned, the full symmetry Raman frequencies obtained from this relaxation, were used to construct the H frequency for the zero point contribution to the enthalpy of these compounds.

LDA formation energies are given in Table III. The formation energies of MgH_2, CaH_2 and SrH_2 are in excellent agreement with experiment and also in good agreement with previous LDA calculations.[29] The formation energy of Mg_2FeH_6 is the best studied of the K_2PtCl_6 hydrides, and is reported as -98 kJ/mol (Ref. 2), -86 kJ/mol (Ref. 7), and -77.4 kJ/mol (Ref. 8). The calculated LDA energy of -133 kJ/mol is significantly larger and this difference would seem to be at the high end of the normal range of LDA errors, especially considering the good agreement with experiment for MgH_2, and FeAl, where we obtain agreement with experiment to within 5 kJ/mol of Fe.[30] Besides LDA errors, the most likely source of error is the crude method that we used to obtain an average phonon frequency. However, even if the average phonon frequency were 250 cm^{-1} higher than our estimate, which we think is unlikely, the calculated enthalpy would shift by only 9 kJ/mol of H_2.

One possibility is that some of the difference is experimental in origin, related to the possible existence of some stable hydride among the decomposition products, which would then stabilize the products relative to Mg_2FeH_6 and therefore would lower the formation energy as measured by the decomposition. In any case, we do find certain trends. First of all, Mg_2FeH_6 is by far the least stable of the K_2PtCl_6 hydrides studied. However, this is connected with the fact that MgH_2 is much less stable than SrH_2 or CaH_2. If one considers formation via $2DH_2 + H_2 + M \rightarrow D_2MH_6$, then this heat of formation is largest for Mg_2FeH_6 as might be expected from an ionic picture. Secondly, the formation energy per H_2 is significantly larger for Mg_2FeH_6 than for MgH_2. This implies that under thermodynamic conditions, without some very unusual entropy contribution, the decomposition should proceed directly to H_2 and the elements, or, at a bare minimum, if there is an intermediate hydride phase, it should not be MgH_2. The formation energies of the Ca and Sr compounds on the other hand are very close to those of CaH_2 and SrH_2, so depending on the conditions, those decompositions may very well proceed via an intermediate $M + DH_2$.

Similar calculations were done for the other compounds in order to estimate the H zero point energy, but these were at a lower level of convergence in the fitting of the dynamical matrix.

VI. STABILITY, BONDING AND IMPLICATIONS

We now speculate about possible implications of our results for hydrogen storage. First of all, we note that the cohesion is ionic, and that it is the Madelung field that stabilizes the $[MH_6]^{4-}$ units. Changes in the Coulomb potential then ought to strongly affect the bond lengths in these units as well as their stability. This is already apparent in the values of x_H of Table I, which show substantial changes in the M-H bond lengths as the lattice parameter is changed by D site substitution (note that the octahedra are not connected so that they need not breath with the lattice). This implies significant tunability in the properties with substitutions. Secondly, the ionic stabilization of the lattice implies that mixed M cation substitutions should be possible and that the octahedral coordination of the metal atoms will be preserved in them. For example, if the partial or full substution Os $\rightarrow \frac{1}{2}$ Re $+ \frac{1}{2}$ Ir could be made, its structure is expected to feature ReH_6 and IrH_6 octahedra, rather than different Re-H and Ir-H coordinations on this lattice. However, it is unclear if any of these substitutions can be made, and even if they can it is unclear whether they will be beneficial. Finally, we note that the fully hydrided compound can therefore be destabilized by driving the transition metal d states up in energy via the Madelung potential, if all other things were equal. One way would be to substitute some fraction of the Mg with a monovalent cation if one can be made to enter the lattice.

However, the stability is relative to the decomposed products, and it is clear from the calculated energetics that these play a major role. For example, Mg_2RuH_6 and Mg_2FeH_6 are the least stable compounds relative to decomposition into elemental Mg and Ru or Fe, but they are the most stable with respect to a hypothetical intermediate MgH_2 + Fe/Ru. As mentioned, this suggests that under normal conditions Mg_2FeH_6 and Mg_2RuH_6 decompose into H_2 and elemental metals without any MgH_2 intermediate, consistent with the observation of Bogdanovic and co-workers.[8]

VII. REDUCING THE FORMATION ENERGY: HYPOTHETICAL Be_2FeH_6

Considering the trend in the energetics with respect to the alkaline earth element, one possibility for obtaining a lower formation energy would seem to be replacement of Mg by Be. This would seem especially likely considering the properties of Be metal, which include strong bonding that would compete with the formation of hydride phases. In order to check this trend we performed calculations for hypothetical Be_2FeH_6 to obtain its formation energy. Since the compound is hypothetical, we obtained the lattice parameter by relaxation in the LDA. The calculated structure has a lattice parameter of 5.65 Å, a H internal coordinate of x=0.2648, and a corresponding

full symmetry Raman phonon frequency of 2233 cm^{-1}. No doubt the LDA underestimates the lattice parameter slightly, as is typical. In any case, with the LDA structure, we obtain a static formation enthalpy of -37 kJ/mol H$_2$ with respect to elemental products. This confirms the conjecture that Be would lead to lower binding energies. However, while this energy suggests that Be$_2$FeH$_6$ would be an interesting hydride phase, it neglects the fact that unlike Mg, Be forms compounds with Fe. In particular, FeBe$_2$ is a known intermetallic compound and would compete with the hydride phase. We calculated the enthalpy of formation of FeBe$_2$ (details are in the next section) and find -87 kJ/mol. The relevant energy for the stability of the hydride Be$_2$FeH$_6$ is therefore not the formation enthalpy from the elements, but from the intermetallic, BeFe$_2$, which, with H$_2$, would be the product of the decomposition. Relative to decomposition into the elements, the existence of the intermetallic then results in a shift of the formation enthalpy of Be$_2$FeH$_6$ by 29 kJ/mol on a per H$_2$ basis, to yield -8 kJ/mol. The average phonon frequency, determined as for the other K$_2$PtCl$_6$ hydrides, discussed above, is 1172 cm^{-1}, yielding a zero point correction of +17kJ/mol H$_2$, placing the calculated enthalpy including zero point at +9 kJ/mol. Thus, it is likely that Be$_2$FeH$_6$ is marginally unstable with respect to decomposition into FeBe$_2$, and therefore will only be formed under high pressure or by chemical routes.

VIII. ELECTRONIC STRUCTURE AND MAGNETISM IN FeBe$_2$

FeBe$_2$ is an interesting hard magnetic material. In particular, it has a relatively low density, high anisotropy and a very high Curie temperature, T_C of 880 K.[35−37] Experimentally, FeBe$_2$ crystallizes in the hexagonal MgZn$_2$ structure (spacegroup $P6_3/mmc$, No. 194) and has magnetization, $M \approx 1.95\mu_B$/Fe. Since we are not aware of previous first principles studies of this material, we briefly summarize our results for the electronic structure of this compound.

The reported lattice parameters are a=4.215 Å, and c=6.853 Å.[35] The unit cell contains four formula units. The Be atoms are on sites 2a (0,0,0) and 6h (x,2x,1/4), while the Fe atoms are on 4f (1/3,2/3,z). Experimental values of the two internal parameters are not available from experiment, so they were found by structural relaxation in the LDA. We find x= 0.8294 and z=0.061. The calculated LDA spin magnetization is 1.76 μ_B/Fe and the magnetic energy is 0.237 eV/Fe. This is only $\sim 3kT_C$ suggesting some itinerant character.

The local spin density approximation (LSDA) band structure and density of states are given in Figures 7 and 8. The band structures shows narrow crystal field split Fe 3d bands on top of a broad manifold of free electron like Be sp derived bands. These Be derived bands are weakly polarized, opposite to the Fe polarization, similar to the case of YFe$_2$, for example.[38,39] The majority spin Fe 3d bands are fully occupied, while the Fermi energy falls in the crystal field gap between the t_{2g} and e_g manifolds in the minority spin. This yields two minority spin e_g holes per Fe, and explains the $\sim 2 \mu_B$/Fe magnetization. Relative to bcc Fe, there is a transfer of Fe s character to the Be derived bands, and a back transfer of charge to give effectively neutral Fe, with eight 3d electrons. This is consistent with the picture discussed by Jesser and Vincze based on experimental susceptibility and Mossbauer measurements.[36] This pseudogapped band structure yields a relatively low density of states at the Fermi energy in both spin channels, $N_\uparrow(E_F)$=0.39 eV^{-1} and $N_\downarrow(E_F)$=0.67 eV^{-1} on a per formula unit basis.

The calculated formation energy of FeBe$_2$ is -87 kJ/mol on a per formula unit basis. As a test of our approach, we also calculated the formation energy of FeAl in the same way. The result was -77 kJ/mol(FeAl), which is in good agreement with the experimental value of -72.6 kJ/mol.[30,40] This suggests that the error in the formation energy of FeBe$_2$ is likely in the range of 5 kJ/mol.

IX. SUMMARY AND DISCUSSION

The present density functional calculations show that the K$_2$PtCl$_6$ hydrides are ionic compounds, with some covalency. The 18 electron rule is a consequence of ligand field effects on the transition metal site. This type of ionic character suggests the possibility of ferroelectricity in related hydrides. We find that the hypothetical compounds, Pb$_2$RuH$_6$ and Be$_2$FeH$_6$ are on the borderline of ferroelectricity, and should be investigated in this context, if they can be made. Further, the ionic character stabilizes H anions, and Fe cations, which is why Fe participates in hydride formation, although Fe metal is not a hydride former. The ionic character implies a certain degree of tunability of the properties of these hydrides, which may allow adjustment of the thermodynamics. However, since Fe and Mg do not form intermetallic compounds, it is likely that the properties of Mg$_2$FeH$_6$ cannot be made better for vehicular H storage than those of MgH$_2$, since MgH$_2$ will be a competing phase.

One way to reduce the stability of the hydride without facing this limitation would be to focus on the stability of decomposition products. One possibility would be to explore minor additions, X that are soluble in and stabilize an Fe-Mg-X intermetallic. These need not enter the hydride lattice, provided that they are available e.g. on hydride particle surfaces to promote the decomposition and provide sufficient enthalpy via the formation of the intermetallic. This may be the most promising avenue for modifying Mg$_2$FeH$_6$ for hydrogen storage applications. As far as we are aware, the solubility of Mg in FeBe$_2$ is

not known. However, if Fe-Be-Mg intermetallics are stable, the present results suggest that the addition of Be to Mg_2FeH_6 may lead to lower stability, which if not for the toxicity of Be, would be favorable for applications.

ACKNOWLEDGMENTS

[1] R.O. Moyer, Jr., C. Stanitski, J. Tanaka, M.I. Kay, and B. Kleinberg, J. Solid State Chem. **3**, 541 (1971).

[2] J.-J. Didisheim, P. Zolliker, K. Yvon, P. Fischer, J. Schefer, M. Gubbelmann, and A.F. Williams, Inorg. Chem. **23**, 1953 (1984).

[3] M. Kritikos, D. Noreus, B. Bogdanovic, and U. Wilczok, J. Less Common Metals **161**, 337 (1990).

[4] B. Huang, F. Bonhomme, P. Selvam, K. Yvon, and P. Fischer, J. Less Common Metals **171**, 301 (1991).

[5] K. Yvon, Chimia **52**, 613 (1998).

[6] R.O. Moyer, Jr., R. Lindsay, and D.F. Storey, Z. Physik Chem. Neue Folge **165**, 83 (1989).

[7] I.G. Konstanchuk, E. Yu. Ivanov, M. Pezat, B. Darriet, V.V. Boldyrev, and P. Hagenmuller, J. Less Common Metals **131**, 181 (1987).

[8] B. Bogdanovic, A. Reiser, K. Schlichte, B. Spliethoff, and B. Tesche, J. Alloys Compd. **345**, 77 (2002).

[9] G.J. Miller, H. Deng, and R. Hoffmann, Inorg. Chem. **33**, 1330 (1994).

[10] D.J. Singh, Phys. Rev. B 53, 176 (1996).

[11] E. Orgaz and M. Gupta, J. Phys. Condens. Matter **5**, 6697 (1993).

[12] D.J. Singh, *Planewaves Pseudopotentials and the LAPW Method* (Kluwer Academic, Boston, 1994).

[13] D. Singh, Phys. Rev. B **43,** 6388 (1991).

[14] S.F. Parker, K.P.J. Williams, M. Bortz, and K. Yvon, Inorg. Chem. **36**, 5128 (1997).

[15] L.F. Mattheiss, Phys. Rev. B **43**, 1863 (1991).

[16] A. Aguayo and D.J. Singh, Phys. Rev. B **69**, 155103 (2004).

[17] A tetrahedral crystal field might also be thought to be favorable as it is also a geometry that is favorable for large large ligand field splittings and hybridization, but in that case only up to 12 electrons would be accomodated – 8 in the 4 H $1s$ orbitals and 4 in the now lower e_g manifold. However, this is not compatible with the electron count of Fe and Mg.

[18] O. Gunnarsson, J. Phys. F **6**, 587 (1976).

[19] H. Yamada, J. Inoue, K. Terao, S. Kanda, and M. Shimizu, J. Phys. F **14**, 1943 (1984).

[20] I.I. Mazin and D.J. Singh, Phys. Rev. B **56**, 2556 (1997).

[21] D.C. Patton, D.V. Porezag, and M.R. Pederson, Phys. Rev. B **55**, 7454 (1997).

[22] E. Wicke and H. Brodowsky, in *Hydrogen in Metals II*, G. Alefeld and J. Volkl, eds, pp 73-155 (Springer-Verlag, Berlin, 1978).

[23] H.-J. Tao, K.-M. Ho, and X.-Y. Zhu, Phys. Rev. B **34**, 8394 (1986).

[24] K. Miwa and A. Fukumoto, Phys. Rev. B **65**, 155114 (2002).

[25] M. Bortz, B. Bertheville, G. Bottger, and K. Yvon, J. Alloys Compd. **287**, L4 (1999).

[26] R. Yu and P.K. Lam, Phys. Rev. B **37**, 8730 (1988).

[27] A.F. Andresen, A.J. Maeland, and D. Slotfeldft-Ellingsen, J. Solid State Chem. **20**, 93 (1977).

[28] N.E. Brese, M. O'Keefe, and R.B. von Dreele, J. Solid State Chem. **88**, 571 (1990).

[29] H. Smithson, C.A. Marianetti, D. Morgan, A. Van der Ven, A. Predith, and G. Ceder, Phys. Rev. B **66**, 144107 (2002).

[30] The most probable source of error is in the magnetic energy of elemental Fe, which is likely underestimated in the LDA. Generalized gradient approximation calculations give a correction of only $\sim$ 5 kJ/mol of H_2; D.J. Singh, W.E. Pickett, and H. Krakauer, Phys. Rev. B **43**, 11628 (1991). The good agreement with experiment for the formation energy of FeAl (which is on the borderline of magnetism) from ferromagnetic Fe and Al supports the conclusion that the error due to the LDA treatment of the magnetic energy of Fe is small.

[31] R.E. Cohen, Nature (London) **358**, 136 (1992).

[32] D.J. Singh and L.L. Boyer, Ferroelectrics **136**, 95 (1992).

[33] The calculated LDA lattice parameters of Pb_2RuH_6 and Sr_2RuH_6 are 14.10 a_0 and 14.17 a_0, respectively, as compared to the experimental lattice parameter of 14.3619 a_0 for Sr_2RuH_6.

[34] M. Fornari and D.J. Singh, Phys. Rev. B **63**, 092101 (2001).

[35] S. Jonsson, K. Kaltenbach, and G. Petzow, Z. Met. **73**, 534 (1982).

[36] R. Jesser and I. Vincze, J. Phys. F: Metal Phys. **6**, 1567 (1976).

[37] H. Samata, Y. Nagata, S. Morita, G. Tanaka, T. Mitsuhashi, S. Yashiro, and S. Abe, J. Alloys Compd. **302**, 29 (2000).

[38] P. Mohn and K. Schwarz, Physica **130B**, 26 (1985).

[39] D.J. Singh and M. Gupta, Phys. Rev. B **69**, 132403 (2004).

[40] J. Breuer, A. Grun, F. Sommer, and E.J. Mittemeijer, Metallurgical and Materials Transactions B **32B**, 913 (2001).

TABLE I. LDA and experimental H positions (x_H(LDA) and x_H(EXP), respectively), fully symmetric A_g Raman frequency, ω, and band gap, E_g.

	x_H(LDA)	x_H(EXP)	ω(cm^{-1})	E_g(eV)
Mg_2FeH_6	0.2412	0.2420 [2]	1923	1.73 X-X
Ca_2FeH_6	0.2257	0.2300 [4]	1759	1.27 X-X
Sr_2FeH_6	0.2178		1694	1.09 Γ-X
Mg_2RuH_6	0.2527	0.2524 [4]	1977	2.93 X-X
Ca_2RuH_6	0.2359		1837	2.29 X-X

Sr_2RuH_6	0.2254	0.223 [1]	1778	2.06 Γ-X
Sr_2OsH_6	0.2262		1893	2.26 Γ-X

TABLE II. LDA and experimental atomic positions (x(LDA), z(LDA) and x(EXP), z(EXP) for $Pnma$ CaH$_2$ and SrH$_2$. y=1/4 for all atoms in this structure.

	x(LDA)	z(LDA)	x(EXP)	z(EXP)
CaH_2 Ca	0.2380	0.1100	0.2378	0.1071 [27]
CaH_2 H1	0.3566	0.4274	0.3573	0.4269 [27]
CaH_2 H2	0.9741	0.6773	0.9737	0.6766 [27]
SrH_2 Sr	0.2382	0.1109	0.2438	0.1108 [28]
SrH_2 H1	0.3558	0.4278	0.3570	0.4281 [28]
SrH_2 H2	0.9732	0.6787	0.9693	0.6825 [28]

TABLE III. LDA energies of formation on a per H$_2$ basis, assuming full decomposition into separated elemental metals and H_2. (minus means that the formation is exothermic). ΔH_{static} denotes the LDA energy with no correction for zero point motion, $\bar{\omega}$ is the average phonon frequency estimated from LDA calculations (see text) and ΔH(kJ mol^{-1}) is the zero-point corrected formation energy for the hydride. The LDA vibrational frequency of H_2 is used in this calculation.

Compound	ΔH_{static}(kJ mol^{-1})	$\bar{\omega}$(cm^{-1})	ΔH(kJ mol^{-1})
Mg_2FeH_6	-147	1089	-133
Ca_2FeH_6	-221	1033	-209
Sr_2FeH_6	-211	871	-205
Mg_2RuH_6	-147	968	-137
Ca_2RuH_6	-229	1013	-218
Sr_2RuH_6	-221	1006	-210
Sr_2OsH_6	-216	1023	-205
MgH_2	-90	954	-81
CaH_2	-219	767	-217
SrH_2	-207	670	-208

TABLE IV. Calculated frequences ω (cm^{-1}) and displacement patterns for zone-center modes of Sr$_2$RuH$_6$, $a = 14.361a_0$ compatible with $R32$ symmetry. The displacements are ($\alpha_{Sr}, \alpha_{Sr}, \alpha_{Sr}$) for the first Sr (in $R32$ symmetry), ($\beta_{Sr}, \beta_{Sr}, \beta_{Sr}$) for the second Sr, ($\gamma_{Ru}, \gamma_{Ru}, \gamma_{Ru}$) for Ru, ($\delta_{H1}, \epsilon_{H1}, \epsilon_{H1}$) for the first type (in $R32$ symmetry) of H (three atoms), and ($\delta_{H2}, \epsilon_{H2}, \epsilon_{H2}$) for the second type of H (three atoms). The δ_H are Ru-H bond stretch coordinates, while ϵ_H are Ru-H bond shears.

ω	α_{Sr}	β_{Sr}	γ_{Ru}	δ_{H1}	ϵ_{H1}	δ_{H2}	ϵ_{H2}
126	0.073	-0.078	0.002	0.001	0.013	0.002	-0.009
141	-0.051	-0.045	0.075	0.075	0.037	0.071	0.041
738	0.003	-0.000	-0.005	-0.024	-0.673	-0.079	0.195
777	-0.002	-0.003	-0.011	-0.087	0.188	-0.012	0.670
1433	0.000	0.000	0.015	-0.632	-0.055	-0.750	-0.020
1742	0.000	0.000	0.002	-0.757	0.012	0.643	-0.044

TABLE V. Phonon frequencies and displacement patterns, as in Table IV but for Pb$_2$RuH$_6$, $a = 14.361a_0$; frequencies, ω are in cm^{-1}.

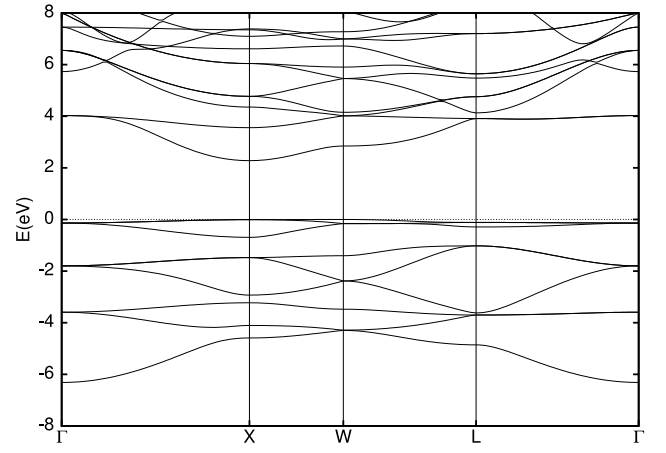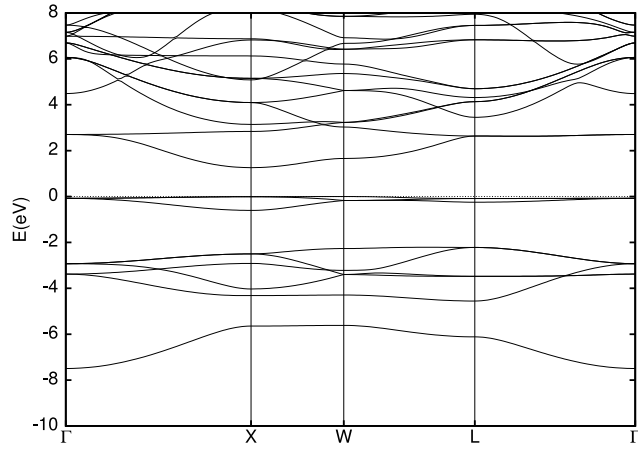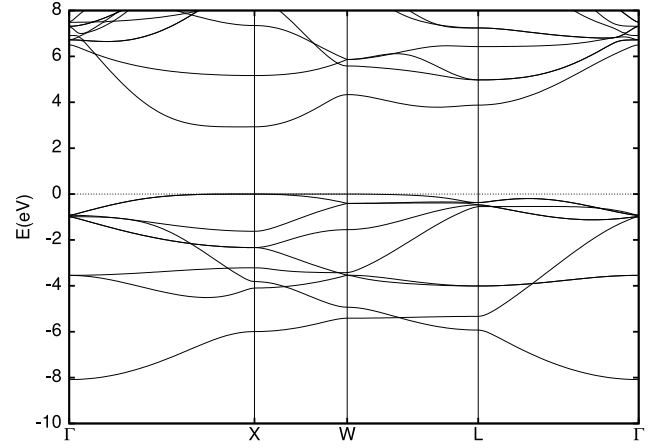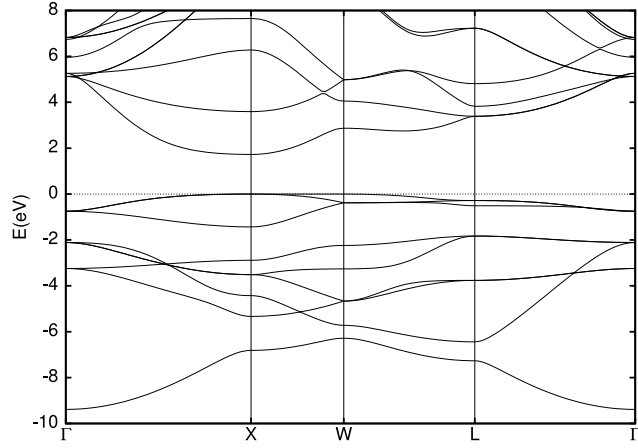| ω	α_{Pb}	β_{Pb}	γ_{Ru}	δ_{H1}	ϵ_{H1}	δ_{H2}	ϵ_{H2}
23	-0.023	-0.019	0.089	0.082	0.038	0.077	0.045
52	0.049	-0.048	0.005	0.005	0.025	0.004	-0.017
552	-0.002	-0.002	-0.010	-0.062	0.518	-0.013	0.469
632	0.002	-0.002	-0.001	-0.022	-0.473	0.041	0.520
1265	0.000	0.000	0.013	-0.646	-0.028	-0.745	-0.008
1626	-0.000	0.000	0.002	-0.749	0.002	0.654	-0.040
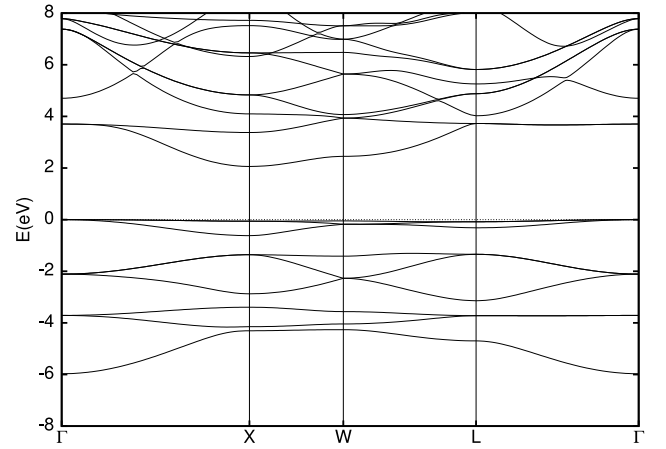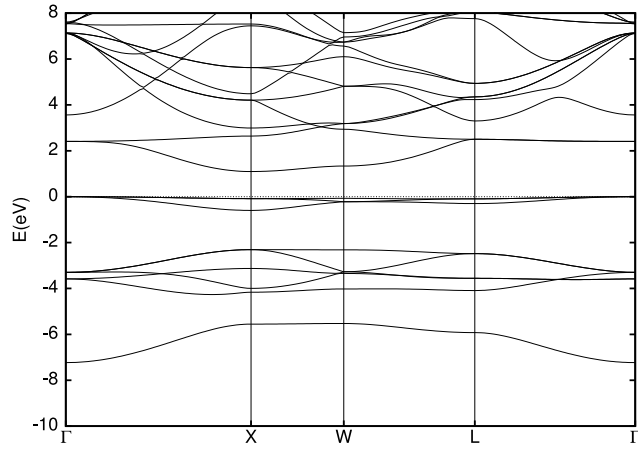
FIG. 1. Band structure of Mg$_2$FeH$_6$ (top), Ca$_2$FeH$_6$ (middle) and Sr$_2$FeH$_6$ (bottom), with the relaxed LDA H positions.

FIG. 2. Band structure of Mg$_2$RuH$_6$ (top), Ca$_2$RuH$_6$ (middle) and Sr$_2$RuH$_6$ (bottom), with the relaxed LDA H positions.
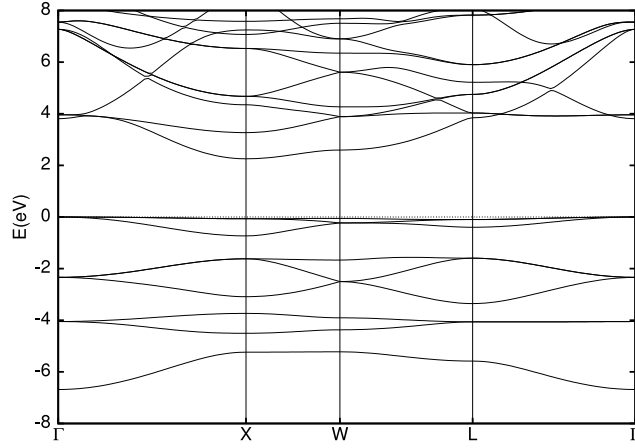
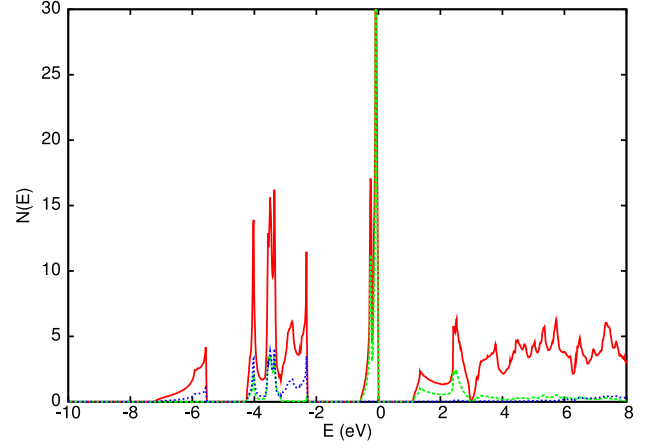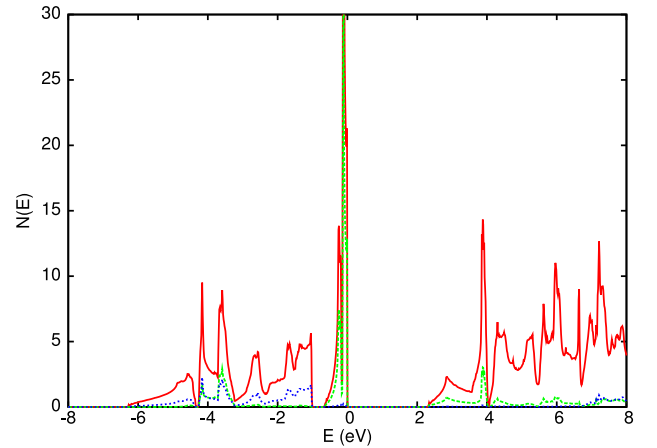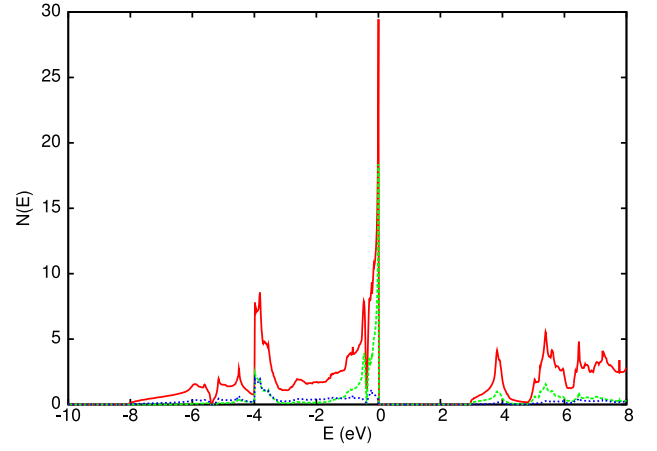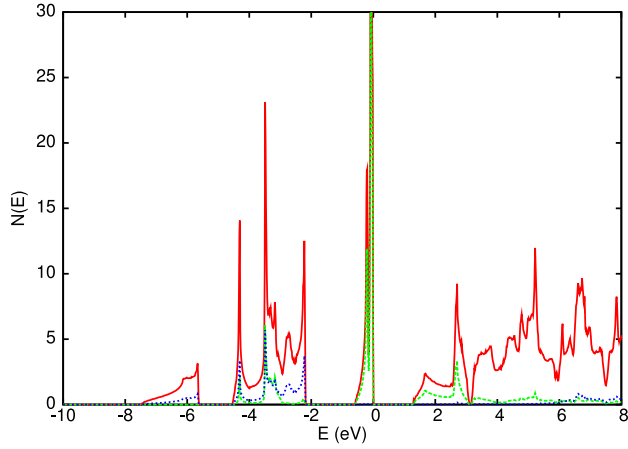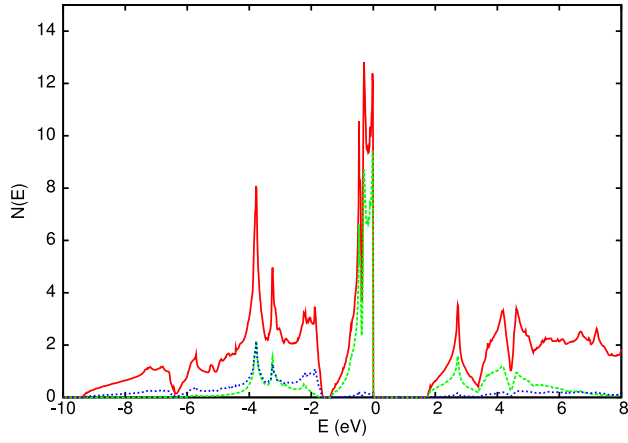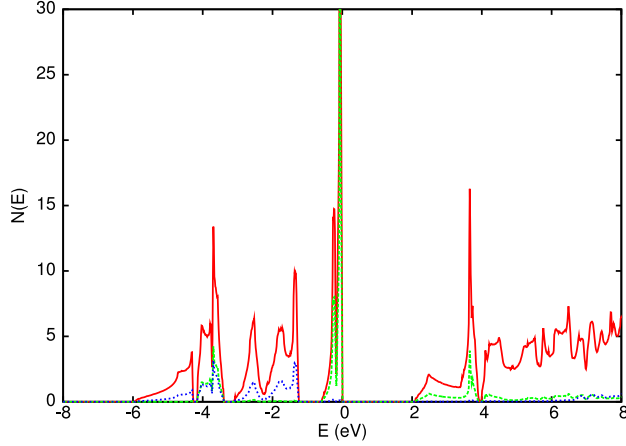FIG. 3. Band structure of Sr_2OsH_6 with the relaxed LDA H positions.

FIG. 4. (color online) Electronic density of states (heavy red line) and projections onto the LAPW spheres of Fe d character (dashed green line) and H s character (dotted blue line) for Mg_2FeH_6 (top),Ca_2FeH_6 (middle) and Sr_2FeH_6 (bottom), with the relaxed LDA H positions, on a per formula unit both spins basis.
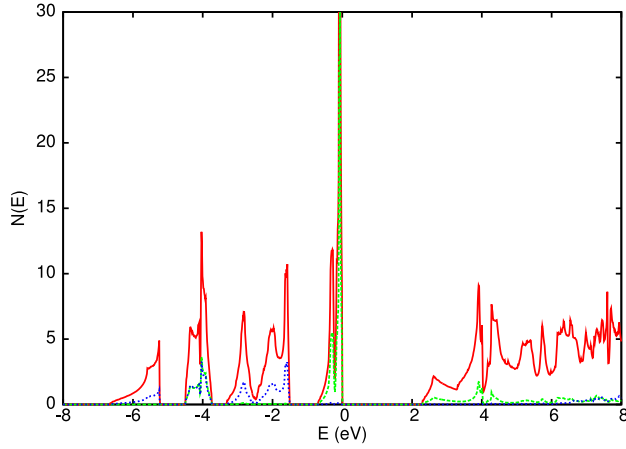
FIG. 5. (color online) Electronic density of states (heavy red line) and projections onto the LAPW spheres of Ru d character (dashed green line) and H s character (dotted blue line) for Mg_2RuH_6 (top), Ca_2RuH_6 (middle), and Sr_2RuH_6 (bottom), with the relaxed LDA H positions, on a per formula unit both spins basis.

FIG. 6. (color online) Electronic density of states (heavy red line) and projections onto the LAPW spheres of Os d character (dashed green line) and H s character (dotted blue line) for Sr_2OsH_6 with the relaxed LDA H positions, on a per formula unit both spins basis.
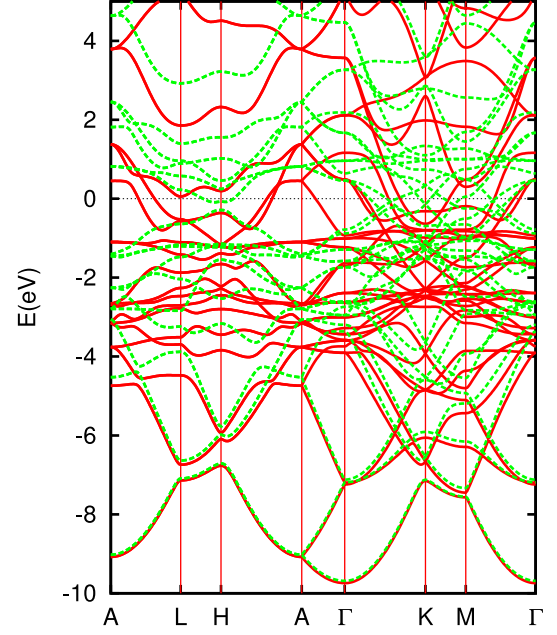

FIG. 7. (color online) Band structure of ferromagnetic $FeBe_2$. Majority (minority) spin bands are given by solid red (dashed green) lines. The Fermi energy is at 0 eV.
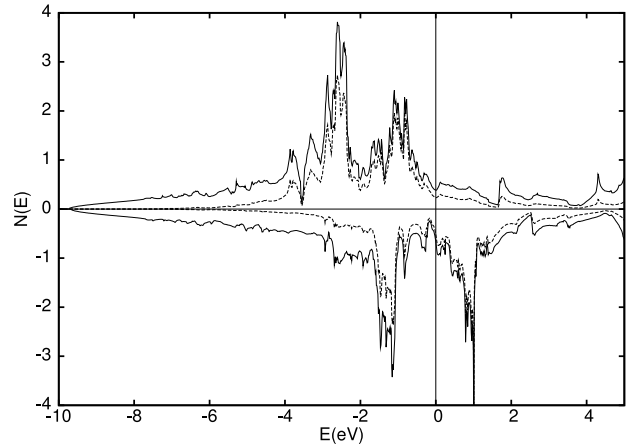

FIG. 8. Electronic density of states (solid) and Fe d projection onto the LAPW sphere (broken, radius 2.1 a_0) for $FeBe_2$ on a per per formula unit basis. Spin-up is above the 0 and spin down is shown as negative. The Fermi level is at 0 eV.